

Contactless electroreflectance study of the Fermi level pinning on GaSb surface in n-type and p-type GaSb Van Hoof structures

R. Kudrawiec, H. P. Nair, M. Latkowska, J. Misiewicz, S. R. Bank et al.

Citation: *J. Appl. Phys.* **112**, 123513 (2012); doi: 10.1063/1.4770413

View online: <http://dx.doi.org/10.1063/1.4770413>

View Table of Contents: <http://jap.aip.org/resource/1/JAPIAU/v112/i12>

Published by the [American Institute of Physics](#).

Related Articles

Electro-optic effect of lithium niobate in piezoelectric resonance

J. Appl. Phys. **112**, 124105 (2012)

Reversible superconductivity in electrochromic indium-tin oxide films

Appl. Phys. Lett. **101**, 252603 (2012)

Optical absorption in highly strained Ge/SiGe quantum wells: The role of $\Gamma \rightarrow \Delta$ scattering

J. Appl. Phys. **112**, 123105 (2012)

Electron spin relaxation in rippled graphene with low mobilities

J. Appl. Phys. **112**, 073709 (2012)

The direct and indirect bandgaps of unstrained $\text{SixGe}_{1-x-y}\text{Sny}$ and their photonic device applications

J. Appl. Phys. **112**, 073106 (2012)

Additional information on J. Appl. Phys.

Journal Homepage: <http://jap.aip.org/>

Journal Information: http://jap.aip.org/about/about_the_journal

Top downloads: http://jap.aip.org/features/most_downloaded

Information for Authors: <http://jap.aip.org/authors>

ADVERTISEMENT



AIP Advances

Now Indexed in
Thomson Reuters
Databases

Explore AIP's open access journal:

- Rapid publication
- Article-level metrics
- Post-publication rating and commenting

Contactless electroreflectance study of the Fermi level pinning on GaSb surface in n-type and p-type GaSb Van Hoof structures

R. Kudrawiec,^{1,2,a)} H. P. Nair,³ M. Latkowska,¹ J. Misiewicz,¹ S. R. Bank,³
 and W. Walukiewicz²

¹*Institute of Physics, Wrocław University of Technology, Wybrzeże Wyspiańskiego 27, 50-370 Wrocław, Poland*

²*Materials Sciences Division, Lawrence Berkeley National Laboratory, Berkeley, California 94720, USA*

³*Microelectronics Research Center, Electrical and Computer Engineering, The University of Texas at Austin, 10100 Burnet Rd., Austin, Texas 78712, USA*

(Received 16 November 2012; accepted 26 November 2012; published online 20 December 2012)

Contactless electroreflectance (CER) has been applied to study the Fermi-level position on GaSb surface in n-type and p-type GaSb Van Hoof structures. CER resonances, followed by strong Franz-Keldysh oscillation of various periods, were clearly observed for two series of structures. This period was much wider (i.e., the built-in electric field was much larger) for n-type structures, indicating that the GaSb surface Fermi level pinning position is closer to the valence-band than the conduction-band. From analysis of the built-in electric fields in undoped GaSb layers, it was concluded that on GaSb surface the Fermi-level is located ~ 0.2 eV above the valence band. © 2012 American Institute of Physics. [<http://dx.doi.org/10.1063/1.4770413>]

I. INTRODUCTION

GaSb is one of the crucial constituents for 6.1 Å lattice system based electronic devices including high electron mobility transistors^{1,2} and semiconductor lasers operating in mid infrared spectral region.^{3–5} One of the fundamental properties affecting the practical applications is the Fermi-level pinning at the (100) GaSb surface (i.e., the surface potential barrier), which is responsible for the formation of Schottky or Ohmic contacts and other phenomena in semiconductor devices. Usually, the surface potential barrier is estimated from electrical measurements using I-V or C-V characteristics of the metal/semiconductor interface. However, the accuracy and reproducibility of this approach are limited because formation of a metal contact on the semiconductor surface influences the surface morphology and thus also the Fermi-level position. Therefore, in order to determine the Fermi-level pinning on a clear semiconductor surface, contactless methods are required.

Contactless electroreflectance (CER) is known as a very powerful method to determine the Fermi-level position in semiconductor structures, including the Fermi-level pinning at the semiconductor surface.^{6–9} So far, there is only a limited number of studies using this technique to investigate GaSb-based heterostructures,^{10,11} and it has not yet been applied to study the Fermi-level pinning at the surface of GaSb material. So far, the issue of Fermi-level position in GaSb system was investigated mostly for metal/GaSb or dielectric/GaSb interface.^{1,2,12} Our method provides a unique opportunity to determine the Fermi level pinning position on a free surface of GaSb.

II. EXPERIMENT

In order to investigate the surface potential barrier for (100) plane of GaSb, n-type and p-type GaSb Van Hoof structures¹³ were grown on (100) GaSb substrates. The surface potential barrier has been determined analyzing the built-in electric field in the undoped GaSb layer of Van Hoof structures. The electric field was determined using the standard approach to analyze the Franz-Keldysh oscillations (FKO).¹⁴ Similar approach was also used recently by us and others to determine electrical field in different material systems.^{6–9,14–18}

GaSb Van Hoof structures of various thicknesses of undoped GaSb top layer (20, 40, and 60 nm) were grown by solid-source molecular beam epitaxy (MBE) in a Varian Gen. II system equipped with a Veeco Mark-IV valved-cracker for antimony and Veeco SUMO effusion cells for gallium and indium. The nominally undoped top layer is p-type with the hole concentration $p < 10^{17} \text{ cm}^{-3}$. Beryllium and tellurium were used as the p-type and n-type dopant, respectively. The n-type ($3 \times 10^{18} \text{ cm}^{-3}$) Van Hoof structures were grown on tellurium-doped (100) ($1-9 \times 10^{17} \text{ cm}^{-3}$) GaSb substrates while the p-type ($3 \times 10^{18} \text{ cm}^{-3}$) Van Hoof structures were grown on unintentionally doped (100) (p-type, $1-9 \times 10^{17} \text{ cm}^{-3}$) GaSb substrates. All samples were grown at a substrate temperature of 460 °C, as measured using a pyrometer. Figure 1 shows schematically the layer sequences in the GaSb Van Hoof structure.

For the CER measurements, the samples were mounted in a capacitor with the top electrode made from a copper-wire mesh which is semi-transparent to light. This electrode was kept at a distance of ~ 0.5 mm from the sample surface, while the sample itself was fixed on the bottom copper electrode. A maximum peak-to-peak alternating voltage of ~ 3.0 kV at a frequency of 285 Hz was applied. Other

^{a)}E-mail addresses: robert.kudrawiec@pwr.wroc.pl and rkudrawiec@lbl.gov.

GaSb Van Hoof structures

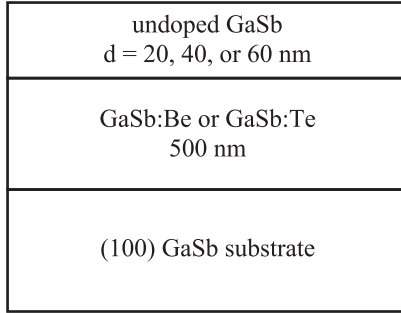


FIG. 1. Schematic diagram of layers in GaSb Van Hoof structures. The electron (hole) concentration in GaSb:Be (GaSb:Te) layer is $3 \times 10^{18} \text{ cm}^{-3}$ ($3 \times 10^{18} \text{ cm}^{-3}$).

relevant details of the CER measurements are described in Refs. 19 and 20. For this study, all CER measurements were performed in ambient air at room temperature.

III. RESULTS AND DISCUSSION

Figure 2 shows room temperature CER spectra for the two sets of GaSb Van Hoof structures. Because of the shallow probing depth of the CER technique²¹ and the architecture of the Van Hoof structures, the entire CER signal can be attributed to the electric field in undoped GaSb layer. CER resonance related the absorption edge at the energy gap of GaSb is clearly observed at $\sim 0.724 \text{ eV}$. This resonance is

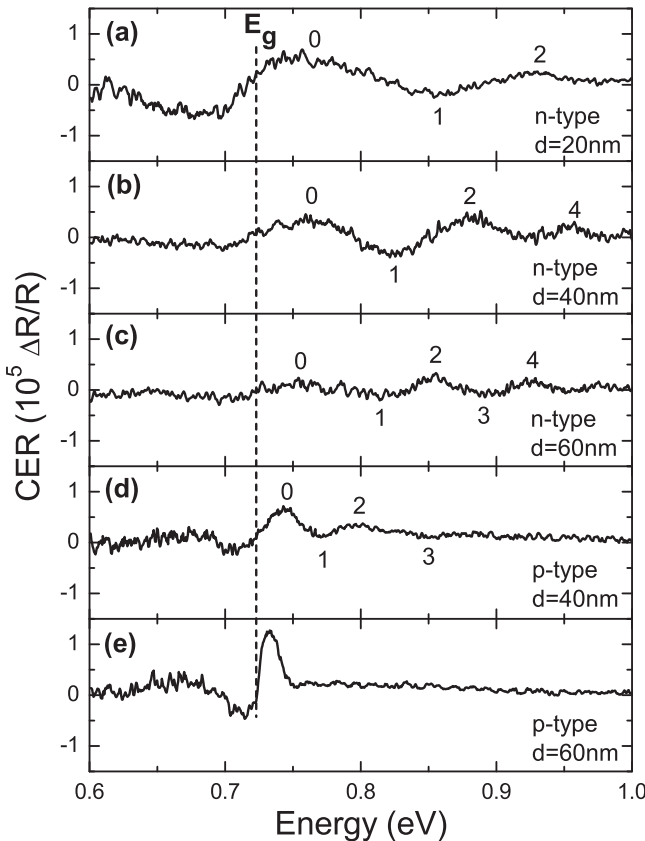


FIG. 2. Room temperature contactless electroreflectance spectra for n-type and p-type GaSb Van Hoof structures of various thicknesses of undoped GaSb layer.

followed by FKO. The period of the FKO is used to estimate built-in electric field. It is assumed that this field is homogeneous since the depletion layer of undoped GaSb is much larger than the thickness of the undoped layer in our samples and, therefore, the built-in electric field in the top GaSb layer is determined from the Fermi level pinning at GaSb surface and the Fermi level position in the doped GaSb layer which is at the edge of the conduction (valence) band for n-type (p-type) structures. A decrease of the built-in electric field is expected when the thickness of the undoped layer is increased. This decrease is clearly observed in Fig. 2 as a shortening of the FKO period. It is worth noting that the whole FKO can be attributed to the optical transitions between the heavy-hole and electron subband. A contribution of light-hole related signal is also expected in CER spectra but its intensity is much weaker and therefore it does not affect the position of FKO extrema. In some samples, the light-hole contribution cannot be neglected especially when more than six FKO extrema are observed, see, for example, Refs. 12 and 13, but for samples studied in this paper only four FKO extrema are analyzed and therefore the light-hole contribution can be neglected.

A conventional method to determine the built-in electric field from the period of FKO is to use an asymptotic expression for the electro-reflectance^{14,22}

$$\frac{\Delta R}{R} \propto \exp \left[\frac{-2\Gamma\sqrt{E-E_g}}{(\hbar\theta)^{3/2}} \right] \cdot \cos \left[\frac{4}{3} \left(\frac{E-E_g}{\hbar\theta} \right)^{3/2} + \varphi \right] \cdot \frac{1}{E^2(E-E_g)}, \quad (1)$$

$$(\hbar\theta)^3 = \frac{e^2 \hbar^2 F^2}{2\mu},$$

where $\hbar\theta$ is the electro-optic energy, Γ is the linewidth, φ is an angle, F is the electric field, and μ is the electron-hole reduced mass which is assumed to be $0.04 m_0$ after Refs. 1 and 23. The extrema of the FKO are given by

$$n\pi = \varphi + \frac{4}{3} \left[\frac{(E_n - E_g)}{\hbar\theta} \right]^{3/2}, \quad (2)$$

where n is the index of the n -th extremum and E_n is the corresponding energy. A plot of $(E_n - E_g)^{3/2}$ versus n yields a straight line with a slope proportional to F .

Figure 3 shows the analysis of the GaSb-related FKO period for the n-type (open points) and p-type (solid points) GaSb Van Hoof structures. Built-in electric fields of 212, 123, and 92 kV/cm were determined for the n-type structures with 20, 40, and 60 nm thick undoped layer, respectively. Much smaller built-in electric fields were found for p-type structures. For the structure with 40 nm thick layer, the field was 54 kV/cm. For p-type structure with 60 nm thick undoped GaSb layer, the built-in electric field was smaller and, therefore, the FKO feature was not clearly observed in CER spectrum. In this case, the CER resonance gives a very good estimate of the GaSb bandgap.

To determine the Fermi-level position at the GaSb surface, the obtained built-in electric fields are plotted in Fig. 4

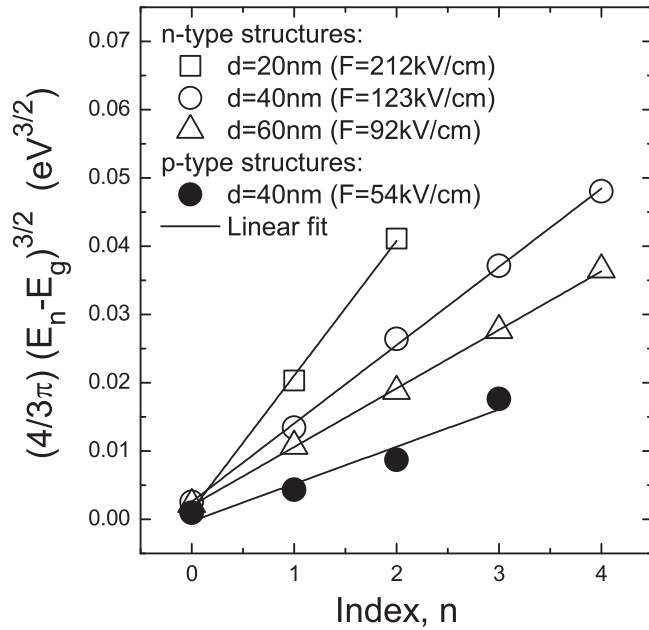


FIG. 3. Analysis of the built-in electric field in the undoped GaSb layer for n-type (open points) and p-type (solid points) GaSb Van Hoof structures.

and fitted by the formula $F = \Phi/d$, with the surface potential barrier Φ treated as a fitting parameter. The best fit for n-type structures was found to be $\Phi = 0.50 \pm 0.05$ eV. The fitting curve is shown by the thick black line in Fig. 4, along with two additional curves corresponding to $\Phi = 0.55$ eV (dashed line) and $\Phi = 0.45$ eV (short dashed line), for a better visualization of the influence of experimental uncertainties on this analysis. In addition, the built-in electric field was also calculated for p-type structures, with the surface potential deter-

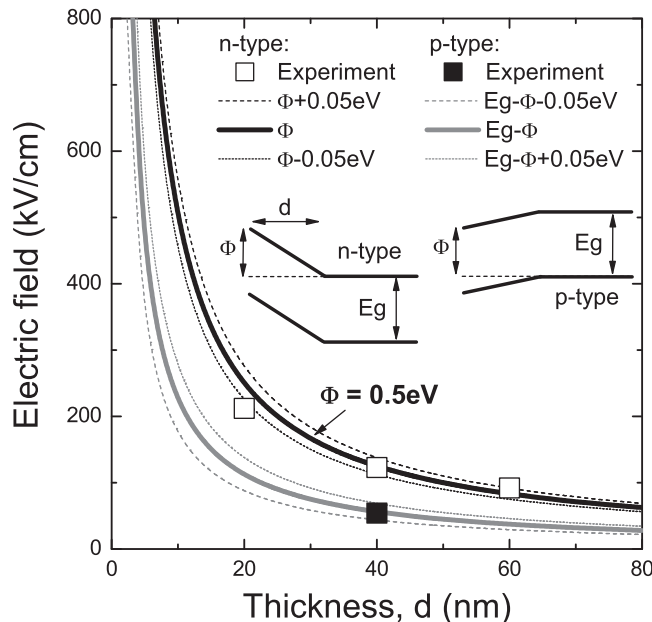


FIG. 4. Built-in electric field determined from FKO analysis for n-type (open squares) and p-type (solid square) GaSb Van Hoof structures. The thick black line is a fit to the open squares, yielding the fitting parameter, $\Phi = 0.50 \pm 0.04$ eV. The thick grey line represents the built-in electric field in p-type GaSb Van Hoof structures for the Fermi level located 0.5 eV below the conduction band.

mined for n-type structures and plotted by grey lines in Fig. 4. It is clearly visible that the surface potential of 0.5 eV very well corresponds to the experimental point determined for the p-type structure with 40 nm thick undoped GaSb layer. The direct analysis of built-in electric field for this sample indicates that the Fermi level pinning position is 0.22 eV above the valence band. It corresponds the surface potential $\Phi = 0.50$ eV, in very good agreement with the analysis for n-type Van Hoof structures. It means that the information obtained from n- and p-type structures is complementary: The electric field for n-type is given by the ratio Φ/d and for p-type is given by $(E_g - \Phi)/d$, as shown in Fig. 4.

The surface Fermi level pinning position for GaSb determined using CER agrees very well with the studies of Folkes *et al.*²⁴ Measuring magnetotransport characteristics for GaSb-InAs-AlSb heterostructures, the authors concluded that the Fermi level is pinned around 0.2 eV above the top of the GaSb valence band when the GaSb cap layer width is greater than 90 nm. For metal/GaSb interface, the Fermi level is located close to the valence band and hence a large n-type Schottky barrier is formed for GaSb structures.^{1,2,12} We believe that the formation of large n-type Schottky barrier for (100) GaSb surface is associated with the intrinsic Fermi level pinning on this surface. It is worth noting that the Fermi level pinning position on (100) GaSb surface measured by us corresponds very well to the Fermi level pinning position in heavily damaged materials, which is known to be located at the so-called “Fermi level stabilization energy” situated ~ 4.9 eV below the vacuum level.²⁵ This suggests that dangling bond like defects tend to stabilize the surface Fermi level at the same energy as in heavily damaged GaSb.

IV. CONCLUSIONS

In conclusion, the Fermi level pinning position on (100) GaSb surface was studied using MBE grown n-type and p-type Van Hoof structures. It has been found that the Fermi level is pinned ~ 0.2 eV above the valence band for both n-type and p-type structures. From the fit of experimental data obtained for the series of n-type structures, the surface potential barrier has been determined to be 0.50 ± 0.05 eV.

ACKNOWLEDGMENTS

R.K. acknowledges for the support within the grant “Mobilnosc Plus” and the Grant No. N N505 485540 from the MNiSzW. Experiments at UT-Austin were supported by the Army Research Office (W911NF-11-1-0521), monitored by Dr. Michael Gerhold. Work at Lawrence Berkeley National Laboratory was supported by the Director, Office of Science, Office of Basic Energy Sciences, Materials Sciences and Engineering Division, of the U.S. Department of Energy under Contract No. DE-AC02-05CH11231.

¹P. S. Dutta, H. L. Bhat, and V. Kumar, *J. Appl. Phys.* **81**, 5821 (1997), and references therein.

²B. R. Bennett, R. Magno, J. B. Boos, W. Kruppa, and M. G. Ancona, *Solid-State Electron.* **49**, 1875 (2005).

- ³A. Bauer, K. Rossner, T. Lehnhardt, M. Kamp, S. Hofling, L. Worschech, and A. Forchel, *Semicond. Sci. Technol.* **26**, 014032 (2011).
- ⁴Z. Yin and X. Tang, *Solid-State Electron.* **51**, 6 (2007).
- ⁵E. Tournié and A. N. Baranov, *Semicond. Semimetals* **86**, 183 (2012).
- ⁶R. Kudrawiec, H. B. Yuen, S. R. Bank, H. P. Bae, M. A. Wistey, J. S. Harris, M. Motyka, and J. Misiewicz, *J. Appl. Phys.* **102**, 113501 (2007).
- ⁷R. Kudrawiec, E. Tschumak, J. Misiewicz, and D. J. As, *Appl. Phys. Lett.* **96**, 241904 (2010).
- ⁸M. Gladysiewicz, R. Kudrawiec, J. Misiewicz, G. Cywinski, M. Siekacz, P. Wolny, and C. Skierbiszewski, *Appl. Phys. Lett.* **98**, 231902 (2011).
- ⁹R. Kudrawiec, M. Gladysiewicz, L. Janicki, J. Misiewicz, G. Cywinski, C. Chèze, P. Wolny, P. Prystawko, and C. Skierbiszewski, *Appl. Phys. Lett.* **100**, 181603 (2012).
- ¹⁰R. Kudrawiec, M. Motyka, J. Misiewicz, M. Hummer, K. Rossner, T. Lehnhardt, M. Muller, and A. Forchel, *Appl. Phys. Lett.* **92**, 041910 (2008).
- ¹¹R. Kudrawiec and J. Misiewicz, *J. Phys.: Conf. Ser.* **146**, 012029 (2009).
- ¹²Z. Yuan, A. Nainani, Y. Sun, J. -Y. J. Lin, P. Pianetta, and K. C. Saraswat, *Appl. Phys. Lett.* **98**, 172106 (2011).
- ¹³C. Van Hoof, K. Deneffe, J. De Boeck, D. J. Arent, and G. Borghs, *Appl. Phys. Lett.* **54**, 608 (1989).
- ¹⁴H. Shen and M. Dutta, *J. Appl. Phys.* **78**, 2151 (1995).
- ¹⁵J. S. Hwang, W. Y. Chou, M. C. Hung, J. S. Wang, and H. H. Lin, *J. Appl. Phys.* **82**, 3888 (1997).
- ¹⁶H. Chouaib, C. Bru-Chevallier, A. Apostoluk, W. Rudno-Rudzinski, M. Lijadi, and P. Bove, *Appl. Phys. Lett.* **93**, 041913 (2008).
- ¹⁷K. I. Lin, H. C. Lin, J. T. Tsai, C. S. Cheng, Y. T. Lu, J. S. Hwang, P. C. Chiu, S. H. Chen, J. I. Chyi, and T. S. Wang, *Appl. Phys. Lett.* **95**, 141914 (2009).
- ¹⁸J. S. Hwang, J. T. Tsai, I. C. Su, H. C. Lin, Y. T. Lu, P. C. Chiu, and J. I. Chyi, *Appl. Phys. Lett.* **100**, 222104 (2012).
- ¹⁹R. Kudrawiec, *Phys. Status Solidi B* **247**, 1616 (2010).
- ²⁰J. Misiewicz and R. Kudrawiec, *Opto-Electron. Rev.* **20**, 101 (2012).
- ²¹M. Motyka, R. Kudrawiec, and J. Misiewicz, *Phys. Status Solidi A* **204**, 354 (2007).
- ²²D. E. Aspnes and A. A. Studna, *Phys. Rev. B* **7**, 4605 (1973).
- ²³I. Vurgaftman, J. R. Meyer, and L. R. Ram-Mohan, *J. Appl. Phys.* **89**, 5815 (2001), and references therein.
- ²⁴P. A. Folkes, G. Gumbs, W. Xu, and W. Xu, *Appl. Phys. Lett.* **89**, 202113 (2006).
- ²⁵W. Walukiewicz, *Physica B* **302–303**, 123 (2001).